Structure *14*, 589–600, March 2006 ©2006 Elsevier Ltd All rights reserved DOI 10.1016/j.str.2005.11.024

Molecular Mechanism for the Regulation of Rho-Kinase by Dimerization and Its Inhibition by Fasudil

Hiroto Yamaguchi,[1,2] Miyuki Kasa,[1,2] Mutsuki Amano,[3] Kozo Kaibuchi,[3] and Toshio Hakoshima[1,2,*]
[1] Structural Biology Laboratory
Nara Institute of Science and Technology
[2] CREST
Japan Science and Technology Agency
8916-5 Takayama
Ikoma
Nara 630-0192
Japan
[3] Department of Cell Pharmacology
Nagoya University
Graduate School of Medicine
65 Tsurumai
Showa
Nagoya
466-8550, Aichi
Japan

Summary

Rho-kinase is a key regulator of cytoskeletal events and a promising drug target in the treatment of vascular diseases and neurological disorders. Unlike other protein kinases, Rho-kinase requires both N- and C-terminal extension segments outside the kinase domain for activity, although the details of this requirement have been elusive. The crystal structure of an active Rho-kinase fragment containing the kinase domain and both the extensions revealed a head-to-head homodimer through the N-terminal extension forming a helix bundle that structurally integrates the C-terminal extension. This structural organization enables binding of the C-terminal hydrophobic motif to the N-terminal lobe, which defines the correct disposition of helix αC that is important for the catalytic activity. The bound inhibitor fasudil significantly alters the conformation and, consequently, the mode of interaction with the catalytic cleft that contains local structural changes. Thus, both kinase and drug conformational pliability and stability confer selectivity.

Introduction

Members of the Rho family of small GTPases act as molecular switches and play pivotal roles in regulating the actin cytoskeleton. Indeed, their activity influences cell polarity, cell adhesion, cytokinesis, neurite retraction, and transcription factor activity (Etienne-Manneville and Hall, 2002). One Rho effector that has received a great deal of attention is Rho-kinase (ROKα, Rho-associated kinase, $p160^{ROCK}$/ROCK II, or ROCK2) (Leung et al., 1995; Matsui et al., 1996; Kimura et al., 1996; Ishizaki et al., 1996). This serine/threonine protein kinase was the first identified target of activated RhoA, and the first role defined for Rho-kinase was to mediate the formation of stress fibers and focal adhesions after RhoA activation (Leung et al., 1996; Amano et al., 1997; Ishizaki et al., 1997). Since then, many contractile processes in smooth muscle and nonmuscle cells have been linked to the Rho/Rho-kinase pathway (Kaibuchi et al., 1999; Riento and Ridley, 2003). Rho-kinase elicits its effect by facilitating myosin light chain (MLC) phosphorylation both directly and indirectly, leading to an increase in phosphorylated MLC. This increase then results in induction of interactions between actin and myosin, thereby enhancing the myosin ATPase activity required for contraction (Amano et al., 1996).

The pathophysiological implications of Rho/Rho-kinase signaling include hypercontraction (abnormal contraction of vascular smooth muscle), which is a major cause of disease such as hypertension and vasospasm of the coronary and cerebral arteries (Fukata et al., 2001). Moreover, abnormal activation of this pathway has been observed in various disorders of the central nervous system (Mueller et al., 2005). Several specific inhibitors of Rho-kinase have been developed to treat these diseases. The isoquinoline derivative fasudil (HA-1077) was one of the first small-molecule inhibitors of Rho-kinase identified (Uehata et al., 1997) and is currently used to clinically treat cerebral vasospasm, a result of subarachnoid hemorrhage (Ono-Saito et al., 1999). Fasudil showed a good selectivity profile toward Rho-kinase in a study that compared its inhibitory effects on 27 serine/threonine kinases (Davies et al., 2000). Rho-kinase inhibitors, including fasudil, have been shown to induce significant vasodilatory effects with a variety of therapeutic indications (Hu and Lee, 2005). Notwithstanding the pronounced importance of the protein in medicine as well as in cell biology, no three-dimensional structure of the kinase domain of Rho-kinase has previously been reported.

Rho-kinase (1388 residues) consists of an N-terminal extension region, a protein kinase domain and its C-terminal extension, a central coiled-coil-forming region encompassing the Rho binding region at its C terminus, and a C-terminal putative pleckstrin homology (PH) domain that includes a cysteine-rich subdomain (Figure 1A). An autoinhibitory mechanism has been proposed for Rho-kinase that involves an intramolecular interaction between the kinase domain and the C-terminal PH domain in the absence of Rho binding (Amano et al., 1999; Chen et al., 2002). Rho-kinase has an isozyme, ROCK1 (also known as ROKβ/ROCK I), that exhibits 92% sequence identity in the kinase domains. The tissue distribution of the two enzymes differs: Rho-kinase is preferentially expressed in brain, whereas ROCK1 shows the highest expression levels in nonneuronal tissues. Rho-kinase displays the greatest homology to myotonic dystrophy kinase (DMPK), DMPK-related cell division control protein 42 (Cdc42) binding kinase (MRCK), and citron kinase (CRIK).

Rho-kinase possesses a novel N-terminal extension to the kinase domain. It has been noted that this extension is required for catalytic activity ever since it was initially identified as an activated RhoA target (Leung et al., 1996) (Figure 1B). Similar N-terminal extensions have

*Correspondence: hakosima@bs.naist.jp

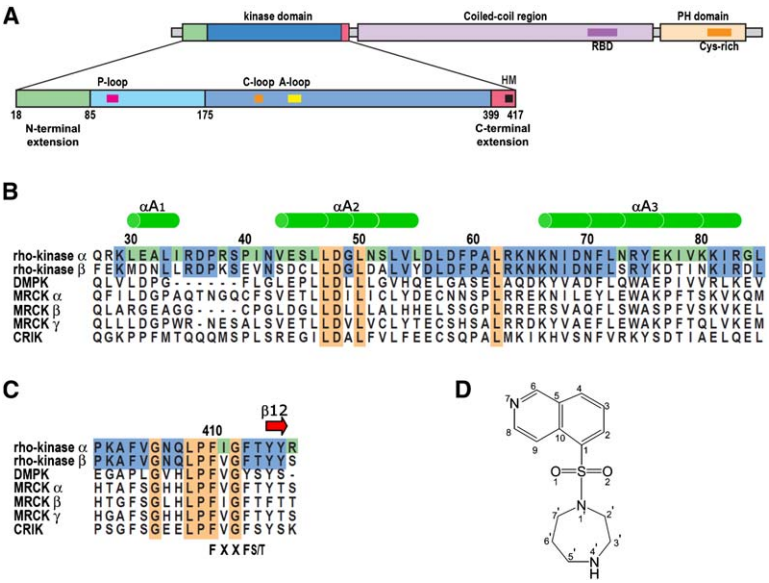

Figure 1. Primary Structure of the Rho-Kinase Extensions

(A) Schematic diagrams of the domains of Rho-kinase. The protein construct used in this study is shown in further detail below: the N-terminal extension is shown in green, the β-rich N-terminal lobe is shown in cyan, the helix-rich C-terminal lobe is shown in blue, and the C-terminal extension is shown in red. Functionally important motifs are indicated inside the domains: RBD for the Rho binding domain, Cys-rich for the putative Zn binding cysteine-rich domain, P loop for the phosphate binding loop (or Glycine-rich loop) with the GxGxϕG motif (magenta), C loop for the catalytic loop (orange), A loop for the activation loop (yellow) and the C-terminal extension (red). The hydrophobic motif (HM) is marked with a black square.

(B) Sequence alignment of the N-terminal extensions of Rho-kinase and the related protein kinases. All sequences are of human origin: Rho-kinase and ROKβ/ROCKI (rho-kinase α and β, respectively), DMPK, three subtypes (α, β, and γ) of MRCK, and citron kinase (CRIK). Leucine and aspartate residues that are conserved among seven kinases are in orange boxes, residues conserved only between Rho-kinases α and β are in blue, and residues conserved among Rho-kinase α proteins from bovine, human, mouse, and rat are in green. Shown above the alignment are the secondary structure elements (α helices, αA_1–αA_3) found in the structure of Rho-kinase.

(C) Sequence alignment of the C-terminal extensions of Rho-kinase and the related protein kinases as in (B). Strand β12, which is found in the Rho-kinase structure, is shown above the alignment.

(D) Chemical structure and atom numbering of fasudil. Fasudil is composed of the planar isoquinoline ring and the pendant ring of seven-membered homopiperazine linked by a sulfonyl group.

been found in MRCK, DMPK, and citron kinase (Bush et al., 2000; Tan et al., 2001; Madaule et al., 1998), but precisely how the N-terminal extension affects catalytic activity remains unknown. Rho-kinase and these related kinases belong to the AGC family of eukaryotic protein kinases, which includes cAMP-dependent protein kinase (PKA), PKG, PKC, PKB/Akt, and PDK1. All of the AGC family members require a C-terminal extension sequence outside the kinase domain for catalytic activity (Peterson and Schreiber, 1999). The C-terminal extension contains a conserved sequence motif of 6 residues, FXXF[T/S][F/Y] (where X represents any amino acid residue) (Figure 1C). This motif is often referred to as the C-terminal "hydrophobic motif," and its binding to the kinase domain is shown to be essential for activity (Pearl and Barford, 2002; Newton, 2003).

Here, we have determined the crystal structure of an active Rho-kinase fragment containing the kinase domain and both the N- and C-terminal extensions in complex with the specific inhibitor, fasudil (Figure 1D). Our structure reveals that the N-terminal extension segments form a novel, to our knowledge, intermolecular helix-bundle fold, the capped helix-bundle (CHB) domain, which brings the two molecules together to form a head-to-head homodimer. This dimer arrangement is consistent with the parallel dimer formation by the coiled-coil domain. The dimerized kinase domain of Rho-kinase appears to be in an active conformation in the absence of phosphorylation. The C-terminal extension is sandwiched between the CHB domain and the kinase domain so that the hydrophobic motif binds the hydrophobic groove on the kinase domain to stabilize the active state. The activation loop adopts an open conformation that allows nucleotide and substrate binding and subsequent catalysis. Thus, we have found direct evidence for the mechanistic significance of the N- and C-terminal extensions to Rho-kinase catalytic activity. We have also uncovered differences in conformation of the bound inhibitor between Rho-kinase and PKA, providing clues for understanding what factors determine specificity.

Results and Discussion

Overview of the Kinase Domain Structure

The protein construct of Rho-kinase used in this study consists of an N-terminal 67 residue extension (residues 18–84) and a kinase domain with a C-terminal extension (residues 85–417) (Figure 1A). The crystal structure of the Rho-kinase fragment complexed with fasudil was determined at 2.4 Å resolution to an R_{cryst} of 19.7% (an R_{free} of 23.5%) (Table 1). Our structure contains two crystallographically independent molecules with similar structures (molecule A and molecule B); the root-mean-square deviation (rmsd) between the two molecules is small (0.65 Å for 321 Cα-carbon atoms). The overall fold of the kinase domain of Rho-kinase is similar to that of other known protein kinases of the AGC family (Figure 2A). The conserved kinase domain shows the canonical protein kinase fold—that is, a bilobal structure with a small N-terminal lobe (residues 85–174) and a larger C-terminal lobe (residues 175–350). The relative disposition of the N- and C-terminal lobes represents a closed form as found in PKA bound to an ATP analog and a PKI peptide (Figures 2B). Fasudil was identified in the interlobe cleft that corresponds to the conserved ATP binding site. The kinase domain of Rho-kinase was best aligned structurally to that of the closed form

Table 1. Crystallographic Data

Diffraction Data[a]	
Wavelength (Å)	0.9000
Space group	$P4_12_12$
Unit cell (Å)	a = b = 102.53, c = 257.19
Resolution (Å)	30.0–2.40 (2.49–2.40)
Unique reflections	52,492
Redundancy	4.96
Completeness	95.8 (81.0)
$I/\sigma(I)$	17.2 (2.14)
R_{sym} (%)	7.5 (34.7)
Refinement Statistics[b]	
Atomic model	
Amino acid residues	769 (for dimer)
Water molecules	162
Fasudil	2
Nonhydrogen atoms	6,411 (for dimer)
Reflections used	452,481
R_{work} (%)	19.7 (28.0)
R_{free} (%)	23.5 (31.6)
Overall B factors (Å^2)	
Protein Molecule A	48.2
Molecule B	46.9
Fasudil	42.0
Water molecules	44.1
All atoms	47.4
Rms deviations	
Bond length (Å)	0.014
Bond angles (°)	1.68
Main chain B factor (Å^2)	1.35

[a] Data for the outermost resolution shell (2.49–2.40 Å) are given in parentheses. Measurements were excluded from scaling and merging when $I/\sigma(I) < 0$.
[b] A subset of data (5%) was excluded from the refinement and was used for the R_{free} calculation.

of PKA (rmsd of 0.86 Å for 193 out of 333 residues) (Figure S1; see the Supplemental Data available with this article online).

The N-terminal lobes of Rho-kinase and PKA consist of common secondary structure elements, a five-stranded β sheet (strands β1–β5) with two α helices (αB and αC), while the C-terminal lobe of Rho-kinase, consisting of eight helices (αD and αI) with seven short strands (β5D–β11), contains three 1 or 2 residue deletion sites and three 4 residue insertion sites (Figure 3). The inserted residues are in close proximity to additional secondary structure elements. The additional β10/β11 strand pair appears at the segment that contains the first and second insertion sites, and the additional helix αGH is located at the loop between helices αG and αH (the αG-αH loop) that contains the third insertion. Another insertion is found in the linker between the kinase domain and the C-terminal extension, which is much longer than that in PKA. The connection (residues 351–398) between the C-terminal lobe and the extension creeps up on the side of the kinase domain from the bottom and crosses over the top of the N-terminal lobe. Finally, residues 388–395 of the connection running above strands β1 and β2 exhibit high temperature factors and show no interpretable electron density in our crystal.

The N-Terminal Extension Mediates Dimerization

The N-terminal extension folds into three α helices (αA_1, αA_2, and αA_3) and is associated with the corresponding part from the adjacent molecule that is related by the crystallographic 2-fold axis (Figures 4A and 4B). The nonpolar contacts around the dyad axis are exemplified by leucine zipper-like interactions between three leucine residues (Leu46, Leu47, and Leu53) on helix αA_2 (Figure 4C). The first half of helix αA_3 is paired with helix αA_2 in an antiparallel manner. Helix αA_3 contains a kink in the middle (at Tyr75), and the rest of the helix is redirected, crossing over helix αA_2, to connect to the N-terminal lobe. The long αA_2 and αA_3 helices run up and down to form a large hydrophobic surface (~1680 Å^2) that interacts with the corresponding helices from the dimerized partner molecule (Figure 4D).

Two short αA_1 helices sit on top of the four-helix bundle formed by helices αA_2 and αA_3 from both protomers (Figure 4B). These helices serve to stabilize the dimerized domain by capping the hydrophobic core of the bundle. Thus, the N-terminal extensions in the dimer structure feature a capped helix-bundle fold, hereafter referred to as the CHB domain. CHB domain-mediated dimerization was clearly demonstrated by the results of gel filtration chromatography, in which the Rho-kinase protein used in our structural study eluted at a retention volume consistent with a dimer, whereas the N-terminal truncated protein (residues 86–417) yielded an elution profile consistent with a monomer (Figure S2A).

Notably, the leucine residues on helices αA_2 are absolutely conserved, not only in Rho-kinase isozymes from different species, but also in MRCK, citron kinase, and DMPK (Figure 1B). In Rho-kinase, the C-terminal extension is directly followed by a long (~700 residues) coiled-coil region (Figure 1A). Both protomers of the dimer point their C termini in the same direction (Figure 4B). This is consistent with the downstream parallel coiled-coil formation indicated by crystal structures of the coiled-coil region fragments (Shimizu et al., 2003; Dvorsky et al., 2004), also implied for MRCK from biochemical studies (Tan et al., 2001). Our dimer structure suggests that full-length active Rho-kinase exists as an entirely parallel dimer (Figure 4E).

The C-Terminal Extension

The most interesting structural aspect of the Rho-kinase dimer is that the very end of the C-terminal extension is situated between the CHB domain and the N-terminal lobe (Figure 4A). The N-terminal half of the extension makes contact more closely with the CHB domain than with the N-terminal lobe, whereas the C-terminal half is sandwiched between the CHB domain and the N-terminal lobe and makes contact with both (Figure 4B). The C-terminal half contains the hydrophobic motif ^{410}FIGFTY^{415} that is completely embedded in the interface.

Three nonpolar residues (Phe403, Leu408, and Ile411) of the N-terminal half of the C-terminal extension poke their hydrophobic side chains into a furrow of the CHB domain, formed by antiparallel helices—αA_2 of one protomer molecule and αA_3 of the other (Figure 5A). These hydrophobic interactions are fortified by polar interactions, namely, the formation of hydrogen bonds between the main chains of the extension and the side chains of the CHB domain, Arg74 from helix αA_3, and Asp48 from helix αA_2. Side chain-to-side chain interactions are also present, consisting of intermolecular

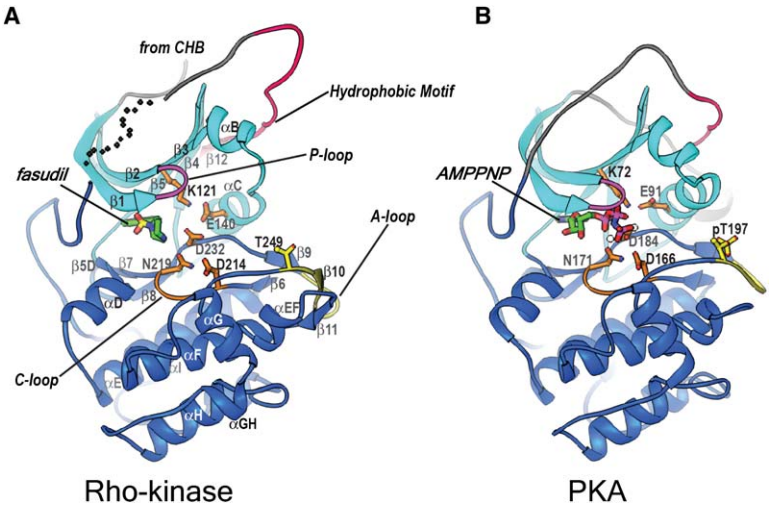

Figure 2. Overall Structure of the Kinase Domain of Rho-Kinase and Comparison with PKA

(A) Ribbon diagram of Rho-kinase (molecules A). The kinase domain with the C-terminal extension is shown in cyan (N-terminal lobe), blue (C-terminal lobe), and red (C-terminal extension containing the hydrophobic motif). The N-terminal extension forming the CHB domain is omitted for clarity. All secondary structure elements are labeled. The bound fasudil is shown as a stick model. Five catalytically important residues (Lys121, Glu140, Asp214, Asn219, and Asp232) in addition to the potential phosphorylation site in the activation loop (Thr249) are shown. The functional motifs are shown with the same color scheme as in Figure 1A; magenta, P loop; orange, C loop; yellow, A loop. Dotted connections between the N-terminal lobe and the C-terminal extension are for residues omitted in model building due to poor electron density (see text).

(B) Ribbon diagram of PKA (PDB code: 1CDK). The bound ATP analog (AMPPNP) is shown as a stick model. Five catalytically important residues (Lys72, Glu91, Asp166, Asn171, and Asp184) and the phosphorylated threonine (pThr197) in the activation loop are shown. The functionally significant motifs are shown with the same color scheme as in (A). The PKI peptide is not shown for clarity.

(Asn406 and Asn67) and intramolecular (Thr414 and Asp48) hydrogen bonds.

On the other side of the C-terminal extension, Pro409 and three aromatic side chains (Phe410, Phe413, and Tyr415) of the hydrophobic motif are anchored to the hydrophobic groove formed by helices αB–αC and strands β4–β5 of the N-terminal lobe (Figure 5B). This fixes, along with a hydrogen bonding network that involves side chains of conserved residues (specifically, Lys125 from helix αB, Arg141 from helix αC, and Glu160 from strand β4), helix αC onto the β sheet. The very end residues, Tyr415 and Tyr416, form a short β strand (β12) next to strand β4 and participate in sheet formation in the N-terminal lobe. The conserved residue Thr414, which is a potential phosphorylation site on the hydrophobic motif in general, has no electron density corresponding to a potential phosphate group (Figure S3). Rather, there is a bridging water molecule between the Thr414 side chain and the main chain amide group of Gln160 from strand β4 of the N-terminal lobe (Figure 5B). Consequently, the C-terminal hydrophobic motif and helix αC are well ordered in our structure.

The CHB domain as a whole statically covers and stabilizes the hydrophobic motif tucked into the hydrophobic groove of the N-terminal lobe. Simultaneously, the C-terminal extension contributes to structural stabilization of the CHB domain, although they are quite distant in the primary sequence (>300 residues). These structural aspects are consistent with a recent hydrodynamic study in which both the N- and C-terminal extensions of Rho-kinase are suggested to be necessary for stable dimer formation (Doran et al., 2004).

The Hydrophobic Motif and Catalytic Activity

In our Rho-kinase structure, the hydrophobic motif bound to the hydrophobic groove on the N-terminal lobe properly aligns helix αC on the β sheet. As a result of this alignment, the conserved Glu140 from helix αC stabilizes catalytically essential Lys121 from strand β3 by ion pairing, as seen in the active form of PKA (Glu91 and Lys72) (Figure 2B). This ion pair (hereafter referred to as the Glu-Lys ion pair), which is a characteristic feature of the active conformation of protein kinases (Huse and Kuriyan, 2002; Newton, 2003; Nolen et al., 2004), enables the lysine residue to extend its side chain amino group toward the binding site for the α- and β-phosphates of ATP, the same site where we find fasudil in our crystal (Figures 2A and 2B). In addition, Ile143 of helix αC stacks onto Phe233 of the conserved Asp-Phe-Gly (DFG) motif to align the conserved residue Asp232 correctly. Thus, structurally embedded in the interface between the CHB domain and the N-terminal lobe, the hydrophobic motif defines helix αC at a proper position for a catalytically active conformation.

Removal of the CHB domain necessarily causes exposure of nonpolar residues (Phe403, Leu408, and Ile411) within the C-terminal extension, and it would destabilize its binding to the hydrophobic groove. In fact, an N-terminally truncated, monomeric protein (residues 86–417) that lacks the CHB domain, but possesses the kinase domain and the C-terminal extension with the hydrophobic motif, has significantly diminished enzymatic activity compared to the dimeric protein used for our structural study (residues 18–417) (Figure S2B). These nonpolar residues in the hydrophobic motif are specific for Rho-kinase and the related kinases requiring their N-terminal extensions for activity, while they are replaced with polar residues in other AGC kinases that do not require their N-terminal extensions. A similar loss of activity was observed for Rho-kinase proteins that lack the C-terminal extension (Doran et al., 2004). The data are consistent with the fact that no extensive, direct interaction between the CHB domain and the N-terminal lobe was observed in our structure. In this way, our structure has successfully addressed the long-standing question of why the N-terminal extension is critical for catalytic activity in Rho-kinase (Leung et al., 1996) as well as in its closely related kinases (Tan et al., 2001).

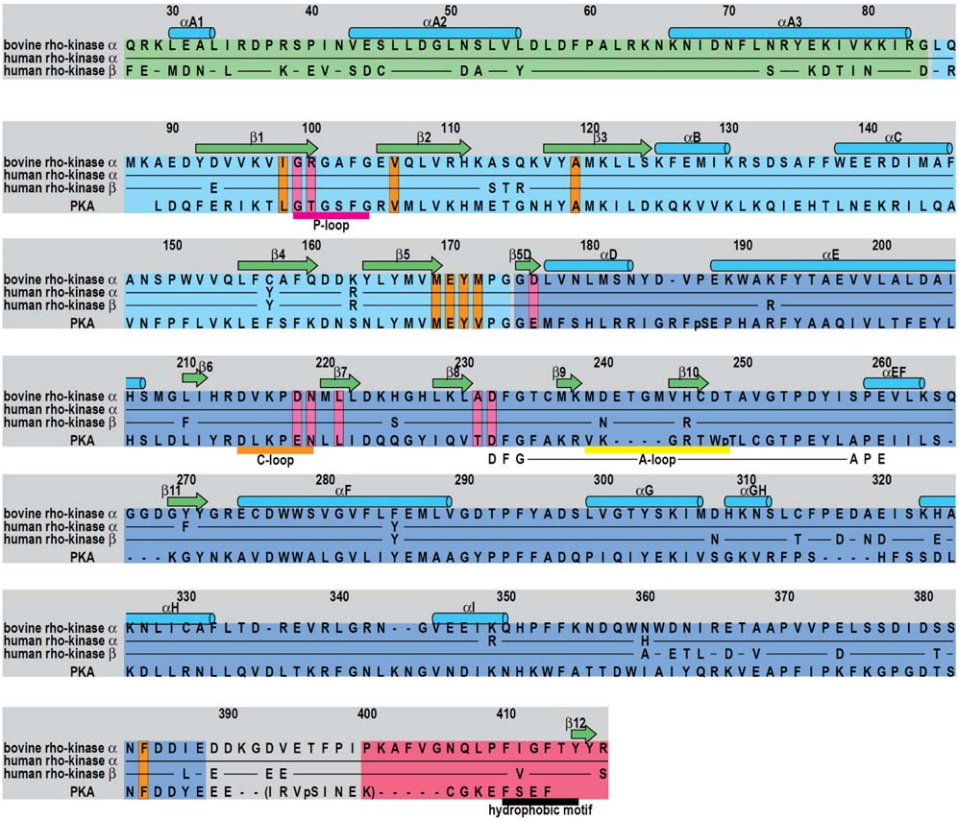

Figure 3. Sequence Alignments of Rho-Kinase and the Related Kinases

The sequences of bovine Rho-kinase and human PKA are aligned based on the structures together with the human ROCK II (Rho-kinase α) and ROCK I (Rho-kinase β) sequences. Shown above the alignment are the secondary structure elements found in the Rho-kinase structure (molecule A); α helices (αA–αI) are shown as blue cylinders, and β sheets (β1–β12) are shown as green arrows with the residue numbering of bovine Rho-kinase. Using the same color scheme as in Figure 1A, functionally important motifs are shown below the alignment. Residues that are in contact with bound fasudil are indicated in orange (positionally conserved between Rho-kinase and PKA, see Experimental Procedures) or magenta boxes (positionally nonconserved).

The Activation Loop

The activation loop shares crucial roles in catalysis with helix αC, which defines formation of the Glu-Lys ion pair and disposition of the DFG motif. Rho-kinase undergoes autophosphorylation (Ishizaki et al., 1996; Matsui et al., 1996) and has a conserved threonine (Thr249) at the central phosphorylation position of the activation loop. In our crystal, Thr249 was not phosphorylated, but the activation loop was moved away from the catalytic center, adopting an open and extended conformation that is permissive for nucleotide and substrate binding and subsequent catalysis (Figure 2A). This ordered conformation resembles the structure of activation loops found in active forms of AGC kinases such as PKA (Figure 2B), suggesting that the conformation of our dimeric Rho-kinase protein exists in an active state. In fact, the catalytic residue Asp214 in the catalytic loop adopts a proper side chain position and conformation by hydrogen bonding to Asn219, as in the active form of PKA (Asp166 and Asn171).

In PKA and most other AGC kinases, the negatively charged, phosphorylated threonine (Thr197 in PKA) of the activation loop is flipped toward the inside. This is anchored by ion pairing with arginine, lysine, and threonine residues (Arg165, Lys189, and Thr195 in PKA) that form an induced-fit positively charged pocket (Figure 5C). In Rho-kinase, the arginine (Arg213) is conserved, but the lysine and threonine residues are replaced with nonpolar residues (Met237 and Cys247) that should fail to interact favorably with the phosphate group. Moreover, helix αC of PKA possesses a histidine side chain (His87) in contact with the phosphate group, whereas this histidine is replaced with Phe136 in Rho-kinase. Therefore, we speculate that anchoring of the phosphate should be weak in Rho-kinase. This could account for the fact that our crystallized Rho-kinase protein was not phosphorylated, although Rho-kinase can undergo autophosphorylation when it is expressed in cells.

In our structure, nonphosphorylated Thr249 protruded somewhat toward the solvent region, while the following P+1 loop virtually adopts the same path as in PKA. We noticed that Rho-kinase possesses two 4 residue insertion sites at or around the activation loop compared with PKA (Figures 3 and 5C). One is ^{241}ETGM^{244}, located in the activation loop, and the other is ^{265}QGGD^{268}, located in the loop between helices αEF and αF (the αEF-αF loop). The former stabilizes an elongated activation loop packed on the latter (the insertion-containing segment) between helices αEF and αF without

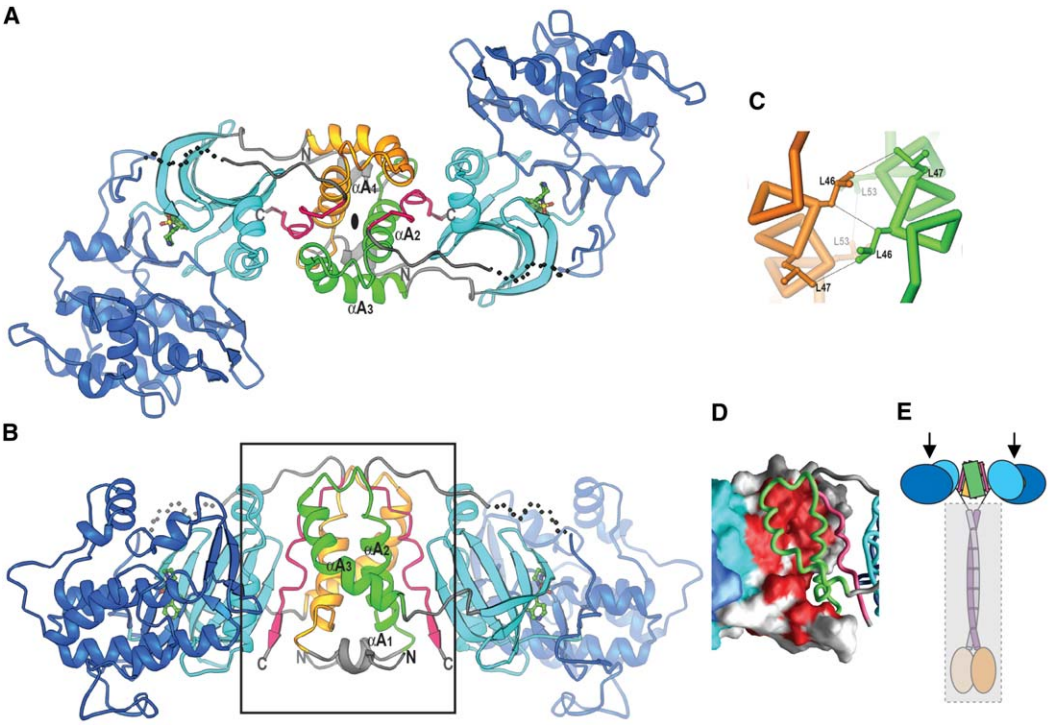

Figure 4. Dimeric Structure of the Rho-Kinase Protein Consisting of the Kinase Domain and the N- and C-Terminal Extensions

(A) Ribbon diagram of the dimer structure of the Rho-kinase protein in the direction looking down the 2-fold axis. The Rho-kinase protein consists of the N-terminal extension (green for one molecule and orange for the other), the kinase domain (cyan for the N-terminal lobe and blue for the C-terminal lobe), and the C-terminal extension (red). The bound inhibitors are shown as stick models.

(B) View of the Rho-kinase dimer in an orthogonal direction as in (A). Both the N and C termini are indicated.

(C) C_α-tracing representation of the leucine zipper-like interaction at the core of the dimer interface. Van der Waals contacts between three leucine residues on helix αA_2 (Leu46, Leu47, and Leu53) are shown.

(D) Close-up view of the dimerization machinery. A region of the CHB domain and the C-terminal extension enclosed in a box in (B) is shown. The dimer interface is drawn as a surface and worm model. In one protomer, the molecular surface of hydrophobic residues from the N-terminal extension helices is colored red.

(E) Schematic diagram of the proposed full-length Rho-kinase structure. Shown on the top is the kinase domains dimerized by the CHB domain as in (B). The following coiled-coil region and the PH domain are also shown in a gray box. Arrows indicate the active sites of the kinase domains, which are facing toward the top.

phosphorylation (Figure 5C). The latter insertion contains 2 glycine residues and creates a bulged cushion to alleviate possible structural stress when strand β11 pairs with strand β10. Our structure implies that phosphorylation of the activation loop is nonessential for the Rho-kinase activation.

Phosphate Binding Loop Plasticity for Fasudil Binding

Fasudil binds to the hydrophobic cleft between the N- and C-terminal lobes of the kinase domain (Figure 2A). The planar isoquinoline ring of fasudil is inserted into the canonical adenine binding pocket of protein kinases, whereas the seven-membered homopiperazine ring is placed at the entrance of the cleft, where active residues are clustered (Figures 6A and 6B). The isoquinoline ring is situated on a hydrophobic platform (Met172, Leu221, and Ala231) and is covered by β sheet residues of the N-terminal lobe (Ile98, Val106, Ala119, and Met169). The edge of the inhibitor ring makes contact with the aromatic rings of Phe384 and Tyr171.

There are a number of contacts between nonpolar side chains of the cleft and the aromatic ring of the inhibitor. We identified 17 residues that have at least 1 atom within a distance of 4 Å from the bound inhibitor (Table S1). Most of these Rho-kinase-inhibitor interactions are conserved in the PKA-fasudil complex (Breitenlechner et al., 2003), although the Rho-kinase residues Ile98, Met172, and Ala231 are replaced with Leu, Val, and Thr, respectively, in PKA (Figure 3). Interestingly, these rather subtle structural variations have a noticeable effect on the positions and conformations of the conserved residues (Figure 6C). Such a variation is exemplified by conserved Leu221, which adopts a stable rotamer by side chain packing with Met172 and Ala231, even though the corresponding Leu of PKA bound to fasudil adopts a rare unstable rotamer configuration (Figure 6D). The stable rotamer of Rho-kinase Leu221 protrudes the terminal methyl group of its side chain toward the inhibitor isoquinoline ring, resulting in an increased number of contacts with the isoquinoline ring (Table S1). This presumably accounts for specificity.

The most interesting aspect of fasudil binding to Rho-kinase is that the homopiperazine rings in our complex differ largely in their disposition and conformation from the corresponding structure in the PKA-fasudil complex, although the inserted isoquinoline ring is fixed in the

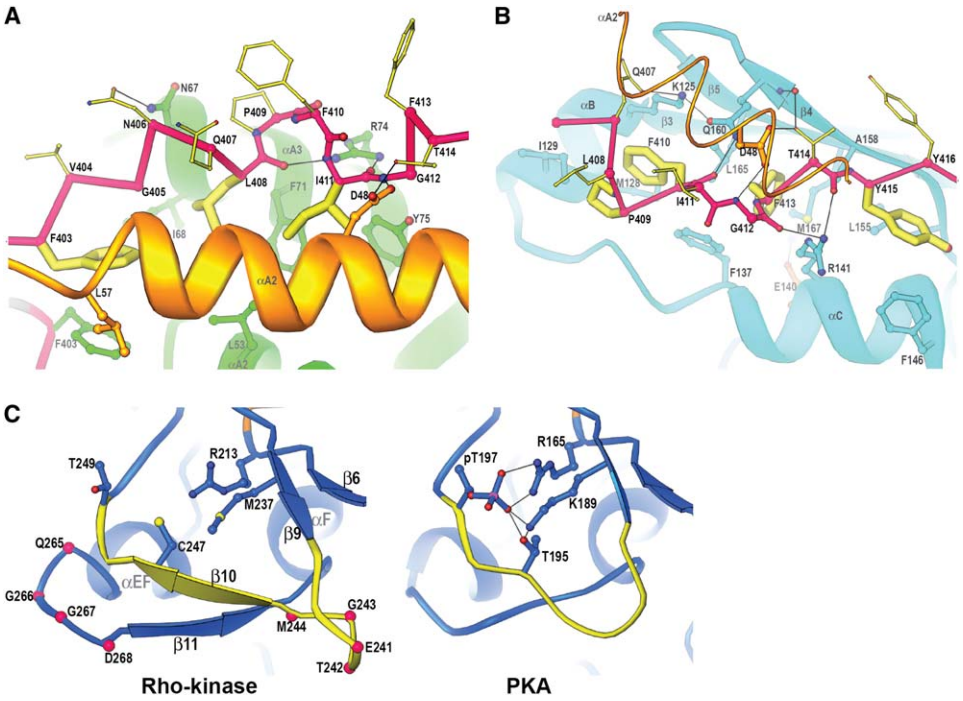

Figure 5. The C-Terminal Extension and the Activation Loop Share Crucial Roles in Catalysis

(A) Graphical representation of the interaction between the C-terminal extension docked to the CHB domain. A main chain trace of the C-terminal extension and ribbons of the CHB domain formed by the N-terminal extension are drawn with the same color scheme as in Figure 4A. The C-terminal extension (red) and helix αA2 (orange) are from the same protomer, while helix αA3 (green) is from the other protomer. The side chains of three nonpolar residues (Phe403, Leu408, and Ile411) of the C-terminal extension are shown as thick stick models in yellow: these hydrophobic side chains dock into a gully of antiparallel helices of the CHB domain. Hydrogen bonds are indicated by thin lines.

(B) Graphical representation of the interaction between the C-terminal extension and the N-terminal lobe of the kinase domain. The hydrophobic motif ^{410}FIGFTY^{415} of the C-terminal extension (red) is docked into the hydrophobic groove of the N-terminal lobe (blue). Three aromatic side chains (Phe410, Phe413, and Tyr415) of the hydrophobic motif and Pro409 are shown as thick stick models in yellow; these fix helix αC onto the β sheet, together with a hydrogen bonding network involving Lys125 from helix αB, Arg141 from helix αC, and Glu160 from strand β4. Thr414 in molecule B forms an additional hydrogen bond with the side chain of Gln160 as well as the hydrogen bonds shown in the figure.

(C) Comparison of the activation segments between Rho-kinase and PKA. Main chain traces of Rho-kinase (molecule A) and PKA (PDB code: 1CDK) are shown along with residues of the activation segment containing the activation loop (yellow). Cα atoms are shown as magenta balls, where Rho-kinase possesses insertions compared with PKA. Residue side chains anchoring phosphorylated Thr197 (PKA) are shown as ball-and-stick models, and hydrogen bonds are indicated as thin lines. The side chains of the corresponding residues and Thr249 in Rho-kinase are also shown. The β10/β11-strand pairing is unique to our Rho-kinase structure, while that in molecule B is somewhat modified, probably as a result of crystal packing (Figure S4).

pocket by the conserved hydrogen bonding between the ring nitrogen atom (N7) and the main chain of Met172 (Figures 7A and 7B). Indeed, replacement of Rho-kinase Asp176 with Glu127 in PKA is likely the major factor accounting for the differences between the Rho-kinase-fasudil and PKA-fasudil complexes. In PKA, the homopiperazine amine group (N4′) is hydrogen bonded to the side chain of Glu127 and the main chain carbonyl group of Glu170. Given the shorter side chain of Asp176, Rho-kinase requires fasudil major conformational changes in order to achieve similar interactions with the amine group (N4′). In molecule A of our complex, the homopiperazine ring shifts from the position seen in PKA to form alternative polar interactions with the side chains of Asn219 and Asp232 (Figure 7A). In molecule B, fasudil shifts the homopiperazine ring resulting from two bond rotations on the central sulfur atom of the sulfonyl group. This conformational change enables the homopiperazine amine group to form hydrogen bonds with the side chain carboxylate of Asp176 and the main chain Asp218 (PKA Glu170) (Figure 7B).

In contrast to the interaction in molecule A, where fasudil is likely to recognize the natural conformation of the Rho-kinase molecule, the interaction with the phosphate binding loop (P loop, or glycine-rich loop) in molecule B appears to involve an induced-fit mechanism (Figures 6A and 6B). The loop of molecule B folds down to increase surface complementarity with the drug. The aromatic ring of Phe103 flips inside the loop to form a number of contacts with the homopiperazine ring, capping the hydrophobic pocket in which the inhibitor binds. This flap is held in place by a hydrogen bond between the main chain carbonyl group of Phe103 at the tip of the loop and the side chain of catalytic Lys121 that forms an ion pair with Glu140 from helix αC (Figure 7C). Interestingly, Asp232 of the DFG motif in molecule B flips up to join Glu140 via ion pairing interactions with Lys121. In contrast, in molecule A, a bridging water molecule between Lys121 and Asp232 occupies the same space that accommodates the side chains of Asp232 and Phe103 in molecule B. Similar water-mediated hydrogen bonds were seen in the PKA-fasudil complex

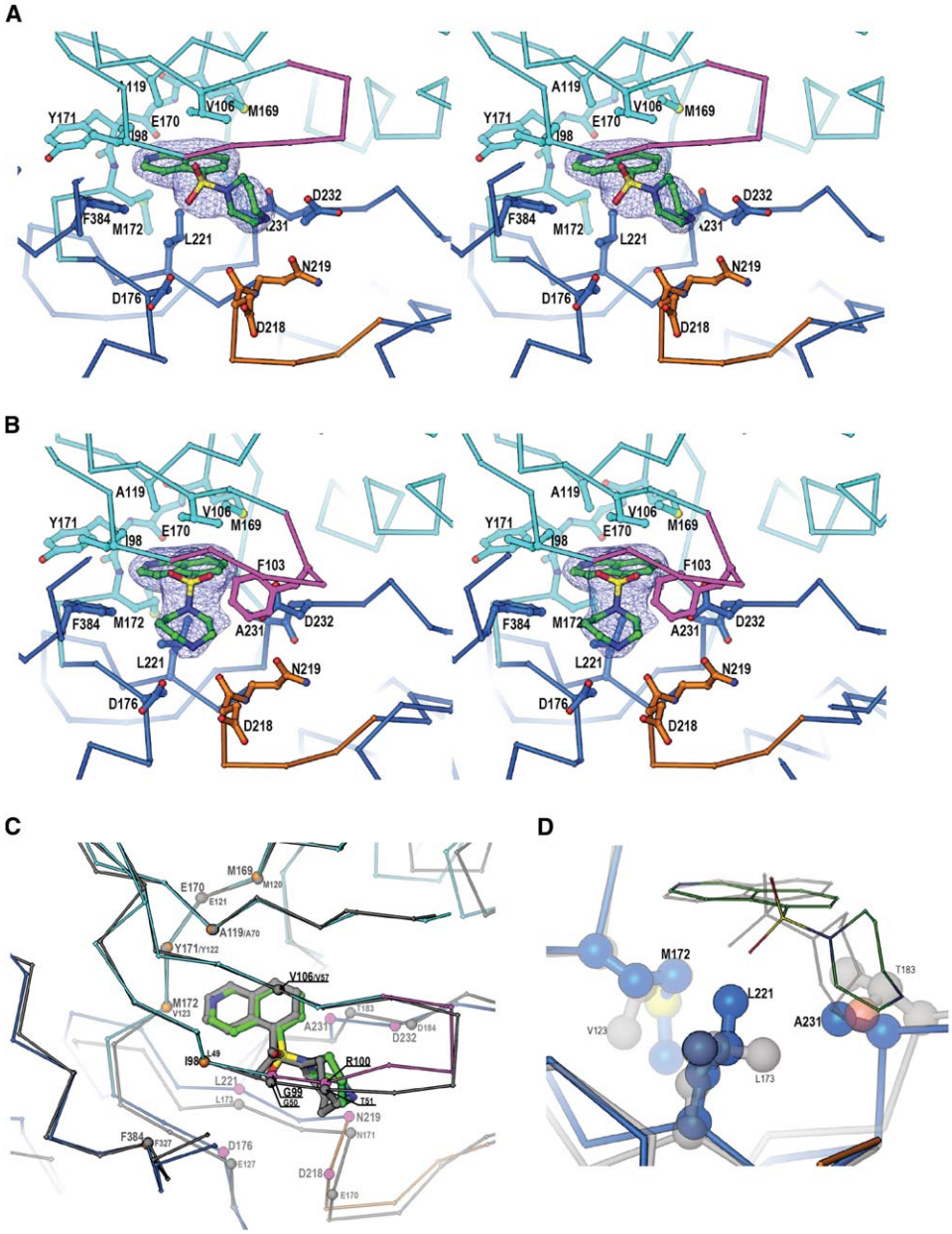

Figure 6. Inhibitor Binding to Rho-Kinase

(A) Stereoview of the nucleotide binding pocket of Rho-kinase molecule A. Residues that interact with fasudil are shown. The inhibitor (carbon atoms in green, oxygen in red, nitrogen in blue, and sulfur in yellow) is shown along with the $F_o - F_c$ electron density map contoured at 2.5σ), which was computed by using phases from a model obtained after simulated annealing with the inhibitor was omitted.

(B) Stereoview of the nucleotide binding pocket of Rho-kinase molecule B. The P loop folds down toward fasudil so that Phe103 makes contact with the pendant ring of the inhibitor (see text). Color codes are as in (A).

(C) Disposition of the Cα atoms of residues in Rho-kinase and PKA in contact with the bound inhibitor fasudil. The backbone Cα traces are shown for the superposed catalytic domains of Rho-kinase (molecule A; same color scheme as in Figure 1) and PKA (PDB code: 1Q8W; gray). Each residue has large and small labels for Rho-kinase and PKA, respectively. The Cα atoms are shown as balls in two colors for Rho-kinase: positionally conserved in orange, and nonconserved in magenta, as in Figure 3.

(D) Rotamer variation found in the fasudil binding sites. The floor of the binding pocket of Rho-kinase (blue) is formed by Met172, Leu221, and Ala23. These residues are superposed with the corresponding residues (Val123, Leu173, and Thr183, respectively) of PKA (gray). The side chains are represented by ball-and-stick models. Leu221 of Rho-kinase adopts a stable rotamer, while the corresponding conserved Leu of PKA bound to fasudil adopts a rare unstable rotamer configuration by side chain packing with nonconserved residues Val123 and Thr183. The stable rotamer of Rho-kinase Leu221 protrudes an increased number of contacts with the isoquinoline ring (Table S1).

and, therefore, would prevent the phosphate binding loop from flipping. The aforementioned conformational change in the inhibitor homopiperazine ring seems to trigger the side chain flip of Asp232 and the large conformational transition of the loop by providing a large space for the Asp232 and Phe103 side chains. As in Rho-kinase, flips of the phosphate binding loop were also found in inhibitor bound protein serine/threonine

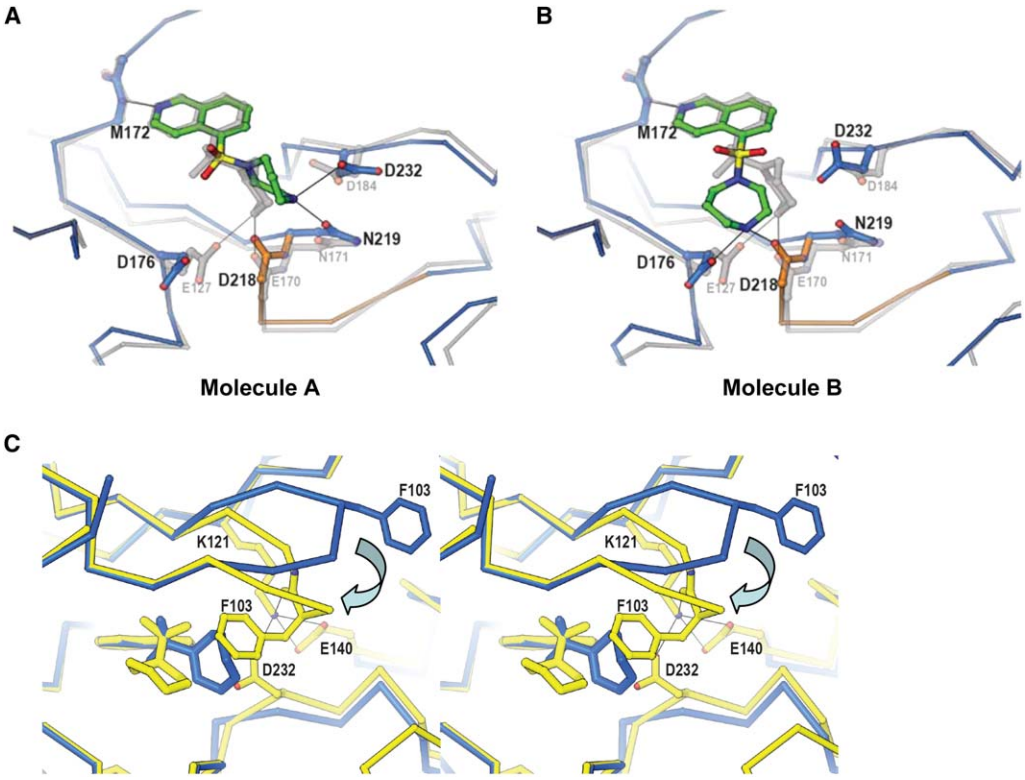

Figure 7. Induced Fit on Inhibitor Binding and the Plasticity of the P Loop

(A) Comparison of fasudil molecules bound to Rho-kinase (molecule A) and PKA (PDB code: 1Q8W). A main chain trace of Rho-kinase (colored as in Figure 4A) is shown along with segments forming the inhibitor binding site containing the residues interacting with the homopiperazine ring of fasudil. A transparent main chain trace of superposed PKA (gray) is also shown along with the residues that interact with the homopiperazine ring. Color codes for the protein and the inhibitor are the same as in Figure 2A. Hydrogen bonds between the inhibitor and the protein are indicated as thin lines. Interaction with different residues in the kinase domain (Asn219 and Asp232 in Rho-kinase; Glu127 and Glu170 in PKA) results in different conformations of the drug pendant rings between the Rho-kinase and the PKA structures.

(B) Comparison of fasudil molecules bound to Rho-kinase (molecule B) and PKA. In Rho-kinase, fasudil shifts the homopiperazine ring due to two bond rotations on the central sulfur atom of the sulfonyl group, comprising an approximate 90° rotation around the bond to the isoquinoline ring, and an approximate 180° rotation around the bond to the pendant ring. These shifts enable the inhibitor in Rho-kinase to form hydrogen bonds with the same residues as in PKA.

(C) Comparison of the Rho-kinase P loops of molecules A (blue) and B (yellow). The P loop of molecule B folds down toward fasudil, and the aromatic ring of Phe103 makes contact with the pendant ring of the inhibitor. The main chain carbonyl group of Phe103 of molecules B is hydrogen bonded to the side chain amino group of the catalytic lysine Lys121 that forms the ion pair with Glu140 and Asp232 of the DFG motif.

kinases (Prade et al., 1997; Gassel et al., 2004) and tyrosine kinases such as FGFR and c-Abl (Mohammadi et al., 1997; Nagar et al., 2003). This loop is known to be mobile in protein kinases, and it can readily accommodate such an induced-fit change upon ligand binding. The phosphate binding loop plasticity in Rho-kinase has the effect of increasing contacts when fasudil binds, which is not seen in the PKA-fasudil complex. This difference between the two kinases' plasticity in the phosphate binding loops may account for the specificity of Rho-kinase for fasudil.

Conclusion

Although the kinase domain of eukaryotic protein kinases shares general structural similarities, regulatory mechanisms that control both catalytic activity and substrate specificity are unique to individual kinases. In this paper, we showed that the dimer-forming N-terminal extension of Rho-kinase folds into the CHB domain, which docks the C-terminal hydrophobic motif onto the N-terminal lobe of the kinase domain. This trapping of the hydrophobic motif by dimerization stabilizes the active state of the kinase domain in the absence of phosphorylation of the hydrophobic motif. Knowledge of this novel, to our knowledge, domain organization in Rho-kinase should facilitate the further development of inhibitors specifically designed to prevent hydrophobic motif trapping. The head-to-head dimerization by the CHB domain is consistent with the previously proposed parallel dimer that forms a coiled coil. The nonphosphorylated activation loop of Rho-kinase adopts virtually the same open conformation as PKA after phosphorylation. This open conformation is stabilized by the extensive interaction between the activation and the αEF-αF loops, both of which have 4 residue insertions compared with PKA. Our observation of the nonphosphorylated kinase domain in an active conformation implies that phosphorylation is nonessential for Rho-kinase activation. A direct structural comparison between the cognate and noncognate complexes defined the specificity-determining mechanisms of the protein kinase inhibitor. Notwithstanding the substantial structural similarity between Rho-kinase and PKA, the proteins exhibit different induced-fit responses of their phosphate binding

loops to fasudil, and conserved residues from each interact quite differently with the bound inhibitor, which as a result, perhaps, adopts different conformations in the two kinases. Understanding these differences in conformational plasticity might help in the development of compounds with improved specificity for treating serious vascular and neuronal diseases.

Experimental Procedures

Protein Expression, Purification, and Crystallization

A recombinant 400 residue fragment (residues 18–417) from Rho-kinase was expressed in Sf9 insect cells with a hexa-histidine tag by using the Bac-to-Bac baculovirus expression system (Life Technologies). The expressed protein was partially purified from the lysate of infected cells on Q-Sepharose XL (Amersham Pharmacia Biotech.) and Ni-NTA Superflow (Qiagen) chromatographic columns at 4ºC. The eluate was concentrated and treated with TEV protease (Parks et al., 1994) at 4ºC for 24 hr to remove the poly-histidine tag. The protein was further purified on Superdex 200 and Q-Sepharose HP columns at 4ºC.

Thin, square, plate-shaped crystals were initially obtained by vapor diffusion at 20ºC in 1–5 μl hanging drops that contained equal volumes of a cocktail solution of 7.73 mg/ml protein and 40 μM fasudil and a reservoir solution of 100 mM sodium citrate (pH 5.0) and 0.8 M sodium citrate. Crystals tended to grow as stacks of many thin plates, and multiple rounds of macroseeding were required to obtain isolated monolithic crystals with increased thickness. Typically, single crystals from the previous cycle were harvested and stored at 20ºC in a solution consisting of the reservoir solution with 5 mM DTT. After 24 hr of storage, the crystals were extensively washed in a solution containing 75 mM sodium citrate (pH 5.0), 0.6 M sodium citrate, and 3.75 mM DTT, and they were seeded into 5 μl of a fresh cocktail solution containing 1.55 mg/ml protein, 60 μM fasudil, 75 mM sodium citrate (pH 5.0), 0.6 M sodium citrate, and 3.75 mM DTT. The seeded protein solution was then equilibrated in a sitting drop against a reservoir solution containing 95 mM sodium citrate (pH 5.0), 0.76 M sodium citrate, and 4.75 mM DTT.

Another construct (residues 86–417) was designed based on the obtained structure of the dimeric Rho-kinase protein so as to omit the N-terminal extension for dimerization. The truncated protein was purified by using the same series of chromatographic columns as the dimer protein. The rsk kinase S6 substrate peptide (RRRLSSLRA) was chemically synthesized.

Structural Determination and Refinement

All of the data were measured from a frozen crystal cryoprotected in 25% (w/v) sucrose. The crystals belong to space group $P4_12_12$, with two molecules of the expressed protein per asymmetric unit, and unit cell dimensions of a = b = 102.53 Å and c = 257.19 Å. A data set was collected at the synchrotron beamline BL44XU at Spring-8 in Japan. Data processing, phase calculation, density modification, and model building were carried out in a standard manner (CCP4, 1994; Kleywegt and Jones, 1997; Otwinowski and Minor, 1997) (Table 1).

The structure was solved by molecular replacement by using Molrep (CCP4, 1994). In selecting an initial search model for molecular replacement, we performed a protein blast search against the PDB entries. The most significant hit was cAMP-dependent protein kinase, PKA (1APM); the second and the third were PKB and PDK1, respectively. The NCS restraints were used on the density modification, but they were not used in the following structural refinement. The structure was improved by simulated annealing with CNS (Brünger et al., 1998) and was refined to 2.4 Å resolution by using REFMAC5 (Murshudov et al., 1999) (Table 1). The current model contains 769 amino acid residues in total. The N-terminal regions (residues 18–26) of both molecules A and B were not included in the final model because of disorder. In addition, a segment of the connection between the C-terminal lobe and the C-terminal extension (residues 389–393 of molecule A and residues 388–395 of molecule B) was not included in the model because of poorly defined electron density. The model also contains 162 water molecules and 2 inhibitor fasudil molecules. The stereochemical quality of the model was monitored by using the program PROCHECK (Laskowski et al., 1993). We have no outliers of the Ramachandran plot, as judged with PROCHECK.

Structural Inspection

As expected from the sequence similarity between Rho-kinase and PKA (39% identity), when a DALI search was performed with our kinase structure, it showed the highest "structural" similarity (Z score of ~36.3) to PKA from among all protein kinase structures compared. To find a better structural alignment, we first superposed the Cα atoms of the catalytic loops (residues 166–171 in PKA and residues 214–219 in Rho-kinase). This was then improved through iterative least-square optimization employing a distance cutoff in which residues were only included when they were in a segment of at least 5 contiguous residues, each of which had a Cα less than 1.5 Å apart from its counterpart. As a result, as much as 58% (193 out of 333 residues) of the Rho-kinase kinase domain was structurally aligned to that of PKA (1Q8W) with an rmsd of 0.86 Å (for molecule A).

In our Rho-kinase structure, we identified 17 residues that have at least one atom within a distance of 4 Å from the bound inhibitor. The Cα dispositions were compared between Rho-kinase and PKA for those residues. The overall superposition of 16 Cα pairs gave an rmsd of 0.56 Å. Three pairs with the smallest Cα deviations were selected, and a strict superposition with these was performed to determine the next closest pair. By repeating this process, we incrementally picked up four more residue pairs (that is, eight pairs in total). Subsequently, the contacting residues were sorted into two subsets based on positional conservation of the Cα atoms with respect to the bound fasudil. The "positionally" conserved subset of 8 residues of Rho-kinase (or of PKA) included Ile98 (Leu49), Val106 (Val57), Ala119 (Ala70), Met169 (Met120), Glu170 (Glu121), Tyr171 (Tyr121), Met172 (Val123), and Phe384 (Phe327) with an rmsd of 0.17 Å. The "positionally" nonconserved 8 residues of Rho-kinase (PKA) included: Gly99 (Gly50), Arg100 (Thr51), Asp176 (Glu127), Asp218 (Glu170), Asn219 (Asn171), Leu221 (Leu173), Ala231 (Thr183), and Asp231 (Asp184). These residues gave an rmsd of 1.04 Å (Figure 6C).

Assay for Catalytic Activity

Kinase reactions with the two fragments of Rho-kinase, residues 18–417 and 86–417, were carried out in 50 μl kinase buffer (50 mM Tris/HCl [pH 7.5], 1 mM EGTA, 1 mM EDTA, 1 mM DTT, and 5 mM $MgCl_2$) containing 100 μM [γ-^{32}P]ATP (1–20 GBq/mmol), the indicated concentrations of recombinant kinases, and 40 μM rsk kinase S6 substrate peptide (RRRLSSLRA). After a 10 min incubation at 30ºC, the reaction mixtures were spotted onto Whatman P81 paper and washed three times with 75 mM phosphoric acid. Incorporation of ^{32}P into the substrate was assessed by scintillation counting.

Supplemental Data

Supplemental Data including a list of protein-fasudil contacts, comparison of overall structures between Rho-kinase and PKA, results of gel filtration and an enzyme assay, the electron density of The414, and comparison of the activation segments between two Rho-kinase molecules are available at http://www.structure.org/cgi/content/full/14/3/589/DC1/.

Acknowledgments

We thank Y. Miwa for preparing gel filtration data and preparing the sample for the enzyme assay; J. Tsukamoto for her technical support in performing MALDI-TOF MS and the N-terminal analysis; and Drs. T. Tsukihara, A. Nakagawa, and E. Yamashita at SPring-8 for use of the synchrotron beamline 44XU. This work was supported in part by a Protein 3000 project on Signal Transduction from the Ministry of Education, Culture, Sports, Science and Technology (MEXT) of Japan (to T.H.).

Received: October 7, 2005
Revised: November 22, 2005
Accepted: November 23, 2005
Published online: March 14, 2006

References

Amano, M., Ito, M., Kimura, K., Fukata, Y., Chihara, K., Nakano, T., Matsuura, Y., and Kaibuchi, K. (1996). Phosphorylation and activation of myosin by Rho-associated kinase (Rho-kinase). J. Biol. Chem. *271*, 20246–20249.

Amano, M., Chihara, K., Kimura, K., Fukata, Y., Nakamura, N., Matsuura, Y., and Kaibuchi, K. (1997). Formation of actin stress fibers and focal adhesions enhanced by Rho-kinase. Science *275*, 1308–1311.

Amano, M., Chihara, K., Nakamura, N., Kaneko, T., Matsuura, Y., and Kaibuchi, K. (1999). The COOH terminus of Rho-kinase negatively regulates rho-kinase activity. J. Biol. Chem. *274*, 32418–32424.

Breitenlechner, C., Gassel, M., Hidaka, H., Kinzel, V., Huber, R., Engh, R.A., and Bossemeyer, D. (2003). Protein kinase A in complex with Rho-kinase inhibitors Y-27632, Fasudil, and H-1152P: structural basis of selectivity. Structure *11*, 1595–1607.

Brünger, A.T., Adams, P.D., Clore, G.M., DeLano, W.L., Gros, P., Grosse-Kunstleve, R.W., Jiang, J.-S., Kuszewski, J., Nilges, M., Pannu, N.S., et al. (1998). Crystallography & NMR system: a new software suite for macromolecular structure determination. Acta Crystallogr. D Biol. Crystallogr. *54*, 905–921.

Bush, E.W., Helmke, S.M., Birnbaum, R.A., and Perryman, M.B. (2000). Myotonic dystrophy protein kinase domains mediate localization, oligomerization, novel catalytic activity, and autoinhibition. Biochemistry *39*, 8480–8490.

CCP4 (Collaborative Computational Project, Number 4) (1994). The CCP4 suite: programs for protein crystallography. Acta Crystallogr. D Biol. Crystallogr. *50*, 760–763.

Chen, X.Q., Tan, I., Ng, C.H., Hall, C., Lim, L., and Leung, T. (2002). Characterization of RhoA-binding kinase ROKα implication of the pleckstrin homology domain in ROKα function using region-specific antibodies. J. Biol. Chem. *277*, 12680–12688.

Davies, S.P., Reddy, H., Caivano, M., and Cohen, P. (2000). Specificity and mechanism of action of some commonly used protein kinase inhibitors. Biochem. J. *351*, 95–105.

Doran, J.D., Liu, X., Taslimi, P., Saadat, A., and Fox, T. (2004). New insights into the structure-function relationships of Rho-associated kinase: a thermodynamic and hydrodynamic study of the dimer-to-monomer transition and its kinetic implications. Biochem. J. *384*, 255–262.

Dvorsky, R., Blumenstein, L., Vetter, I.R., and Ahmadian, M.R. (2004). Structural insights into the interaction of ROCKI with the switch regions of RhoA. J. Biol. Chem. *279*, 7098–7104.

Etienne-Manneville, S., and Hall, A. (2002). Rho GTPases in cell biology. Nature *420*, 629–635.

Fukata, Y., Amano, M., and Kaibuchi, K. (2001). Rho-Rho-kinase pathway in smooth muscle contraction and cytoskeletal reorganization of non-muscle cells. Trends Pharmacol. Sci. *22*, 32–39.

Gassel, M., Breitenlechner, C.B., König, N., Huber, R., Engh, R.A., and Bossemeyer, D. (2004). The protein kinase C inhibitor bisindolyl maleimide 2 binds with reversed orientations to different conformations of protein kinase A. J. Biol. Chem. *279*, 23679–23690.

Hu, E., and Lee, D. (2005). Rho kinase as potential therapeutic target for cardiovascular diseases: opportunities and challenges. Expert Opin. Ther. Targets *9*, 715–736.

Huse, M., and Kuriyan, J. (2002). The conformational plasticity of protein kinases. Cell *109*, 275–282.

Ishizaki, T., Maekawa, M., Fujisawa, K., Okawa, K., Iwamatsu, A., Fujita, A., Watanabe, N., Saito, Y., Kakizuka, A., Morii, N., and Narumiya, S. (1996). The small GTP-binding protein Rho binds to and activates a 160 kDa Ser/Thr protein kinase homologous to myotonic dystrophy kinase. EMBO J. *15*, 1885–1893.

Ishizaki, T., Naito, M., Fujisawa, K., Maekawa, M., Watanabe, N., Saito, Y., and Narumiya, S. (1997). $p160^{ROCK}$, a Rho-associated coiled-coil forming protein kinase, works downstream of Rho and induces focal adhesions. FEBS Lett. *404*, 118–124.

Kaibuchi, K., Kuroda, S., and Amano, M. (1999). Regulation of the cytoskeleton and cell adhesion by the Rho family GTPases in mammalian cells. Annu. Rev. Biochem. *68*, 459–486.

Kimura, K., Ito, M., Amano, M., Chihara, K., Fukata, Y., Nakafuku, M., Yamamori, B., Feng, J., Nakano, T., Okawa, K., et al. (1996). Regulation of myosin phosphatase by Rho and Rho-associated kinase (Rho-kinase). Science *273*, 245–248.

Kleywegt, G.J., and Jones, T. (1997). Model building and refinement practice. Methods Enzymol. *277*, 208–230.

Laskowski, R.A., MacArthur, M.W., Moss, D.S., and Thornton, J.M. (1993). PROCHECK: a program to check the stereochemical quality of protein structures. J. Appl. Crystallogr. *26*, 283–291.

Leung, T., Manser, E., Tan, L., and Lim, L. (1995). A novel serine/threonine kinase binding the Ras-related RhoA GTPase which translocates the kinase to peripheral membranes. J. Biol. Chem. *270*, 29051–29054.

Leung, T., Chen, X.Q., Manser, E., and Lim, L. (1996). The p160 RhoA-binding kinase ROKα is a member of a kinase family and is involved in the reorganization of the cytoskeleton. Mol. Cell. Biol. *16*, 5313–5327.

Madaule, P., Eda, M., Watanabe, N., Fujisawa, K., Matsuoka, T., Bito, H., Ishizaki, T., and Narumiya, S. (1998). Role of citron kinase as a target of the small GTPase Rho in cytokinesis. Nature *394*, 491–494.

Matsui, T., Amano, M., Yamamoto, T., Chihara, K., Nakafuku, M., Ito, M., Nakano, T., Okawa, K., Iwamatsu, A., and Kaibuchi, K. (1996). Rho-associated kinase, a novel serine/threonine kinase, as a putative target for small GTP binding protein Rho. EMBO J. *15*, 2208–2216.

Mohammadi, M., McMahon, G., Sun, L., Tang, C., Hirth, P., Yeh, B.K., Hubbard, S.R., and Schlessinger, J. (1997). Structures of the tyrosine kinase domain of fibroblast growth factor receptor in complex with inhibitors. Science *276*, 955–960.

Mueller, B.K., Mack, H., and Teusch, N. (2005). Rho kinase, a promising drug target for neurological disorders. Nat. Rev. Drug Discov. *4*, 387–398.

Murshudov, G.N., Vagin, A.A., Lebedev, A., Wilson, K.S., and Dodson, E.J. (1999). Efficient anisotropic refinement of macromolecular structures using FFT. Acta Crystallogr. D Biol. Crystallogr. *55*, 247–255.

Nagar, B., Hantschel, O., Young, M.A., Scheffzek, K., Veach, D., Bornmann, W., Clarkson, B., Superti-Furga, G., and Kuriyan, J. (2003). Structural basis for the autoinhibition of c-Abl tyrosine kinase. Cell *112*, 859–871.

Newton, A.C. (2003). Regulation of the ABC kinases by phosphorylation: protein kinase C as a paradigm. Biochem. J. *370*, 361–371.

Nolen, B., Taylor, S., and Ghosh, G. (2004). Regulation of protein kinases: controlling activity through activation segment conformation. Mol. Cell *15*, 661–675.

Ono-Saito, N., Niki, I., and Hidaka, H. (1999). H-series protein kinase inhibitors and potential clinical applications. Pharmacol. Ther. *82*, 123–131.

Otwinowski, Z., and Minor, W. (1997). Processing of X-ray diffraction data collected in oscillation mode. Methods Enzymol. *276*, 307–326.

Parks, T.D., Leuther, K.K., Howard, E.D., Johnston, S.A., and Dougherty, W.G. (1994). Release of proteins and peptides from fusion proteins using a recombinant plant virus proteinase. Anal. Biochem. *216*, 413–417.

Pearl, L.H., and Barford, D. (2002). Regulation of protein kinases in insulin, growth factor and Wnt signalling. Curr. Opin. Struct. Biol. *12*, 761–767.

Peterson, R.T., and Schreiber, S.L. (1999). Kinase phosphorylation: keeping it all in the family. Curr. Biol. *9*, R521–R524.

Prade, L., Engh, R.A., Girod, A., Kinzel, V., Huber, R., and Bossemeyer, D. (1997). Staurosporine-induced conformational changes of cAMP-dependent protein kinase catalytic subunit explain inhibitory potential. Structure *5*, 1627–1637.

Riento, K., and Ridley, A.J. (2003). Rocks: multifunctional kinases in cell behaviour. Nat. Rev. Mol. Cell Biol. *4*, 446–456.

Shimizu, T., Ihara, K., Maesaki, R., Amano, M., Kaibuchi, K., and Hakoshima, T. (2003). Parallel coiled-coil association of the RhoA-binding domain in Rho-kinase. J. Biol. Chem. *278*, 46046–46051.

Tan, I., Seow, K.T., Lim, L., and Leung, T. (2001). Intermolecular and intramolecular interactions regulate catalytic activity of myotonic dystrophy kinase-related Cdc42-binding kinase α. Mol. Cell. Biol. *21*, 2767–2778.

Uehata, M., Ishizaki, T., Satoh, H., Ono, T., Kawahara, T., Morishita, T., Tamakawa, H., Yamagami, K., Inui, J., Midori Maekawa, M., and Narumiya, S. (1997). Calcium sensitization of smooth muscle mediated by a Rho-associated protein kinase in hypertension. Nature *389*, 990–994.

Accession Numbers

Atomic coordinates and structure factor amplitudes of the Rho-kinase-fasudil complex have been deposited in the Protein Data Bank under accession code 2F2U.